

Fiber Bragg Grating Arrays in All-Solid Photonic Bandgap Fiber

Tingting Han and Jingping Yang

Abstract The fiber Bragg grating arrays are inscribed into the Ge-doped cladding rods in an all-solid photonic bandgap fiber. Different resonance wavelengths and widths are observed by launching light into different rods from two reverse directions. The diverse resonance dips from different rods may have different responses to the environment changes, hence the fiber Bragg grating arrays will have good capacity to be employed as the multi-parameter sensor.

Keywords Photonic crystal fiber • Fiber Bragg gratings • Multi-parameter sensor

1 Introduction

The photonic bandgap fiber (PBGF) as a specific photonic crystal fiber (PCF) [1, 2] guides light in the low index core through photonic bandgap effect. In recent years, many researchers pay more attention to the all-solid PBGFs [3], which are composed of a two-dimensional periodic array of high-index rods embedded in a low-index background and a low-index core formed by omitting one or more rods. The all-solid PBGFs have more advantages of easy fabrication, convenience to splice to the conventional single mode fiber (SMF) and no surface mode excited, compared with the hollow-core PBGFs. Moreover, the fiber core and the fiber cladding rods can be doped for fiber Bragg grating (FBG) inscription by UV illumination. Jin et al. [4, 5] realized a fiber Bragg grating photoinscribed into the Ge-doped cladding rods in an all-solid PBGF and observed the resonances between the guided core mode and the guided LP₀₁ supermode. Bigot et al. [6] realized the fiber Bragg grating with reflectivity up to 25 dB, photo-written in the Ge-doped core of a 2D all-solid PBGF. Cook et al. [7] demonstrated the successful inscription

T. Han (✉) · J. Yang
College of Electronic and Communication Engineering,
Tianjin Normal University, Tianjin 300387, China
e-mail: hanting608@163.com

of Bragg gratings in the germanium rings of Yb^{3+} -doped photonic bandgap fiber, and reflection bands were observed from the guided modes of the concentric annular rings, rather than from the core mode.

In this letter, the fiber Bragg grating arrays are realized by inscribing into the Ge-doped cladding rods in an all-solid PBG hydrogen loaded fiber using the KrF excimer laser. The resonance dips are observed only if the light is launched into the Ge-doped cladding rods. When the light is launched into the all-solid PBGF and then passed through the FBG, there will be two kinds of mode couplings. The one kind is the coupling occurring between the adjacent rods of the all-solid PBGF when light is traveling through the all-solid PBGF, and the other kind is the coupling to the reversed guided supermode in the cladding rods of the PBGF when light is traveling through the FBG. Then we launch the light into the Ge-doped rods from two reverse directions, in other words, the light travels through different lengths in the PBGF before passing through the FBG, different resonance wavelengths and the resonance width are observed.

2 Experimental Setup

The microscope image of the all-solid PBGF used in our experiment, which was fabricated by Yangtze Optical Fiber and Cable Company Ltd of China, is shown in the inset of Fig. 1b. Five layers high-index rods (germanium doped) with single rod surrounded by an index depressed layer (fluorine doped) are embedded in the pure silica background. The core is formed by omitting a high-index rod and a low-index ring. The diameter of the fiber is 125 μm , and the distance between the adjacent rods Λ is 10 μm . The outer diameters of the high-index rod and the low-index ring are 0.3786 Λ and 0.7572 Λ , respectively. Compared with the pure silica background, the average refractive index difference of the high-index rods and the low-index rings are 0.034 and -0.08 , respectively.

A 1.5 m all-solid PBGF, with 3 cm section which is stripped the coating at the distance of 9 cm from the beginning end, is loaded in a hydrogen atmosphere at 100 atm, 100 $^{\circ}\text{C}$ for 48 h to enhance its photosensitivity. Then the stripped section is exposed by focused pulses from a 248 nm KrF excimer laser with average energy of single pulse of 40 mJ at a repetition rate of 2 Hz for 2 min. The grating period is 593 nm. The FBG is fabricated, as shown in the right part of Fig. 1b. A broadband source covering from 1520 nm to 1580 nm passing through the SMF is coupled into the core and the Ge-doped rods of the all-solid PBGF. An ANDO Q8383 optical spectrum analyzer is connected to the other end of the all-solid PBGF for measuring transmission spectrum of the FBGs, as shown in Fig. 1a. Figure 1b is a blow up of the section circled by the dotted ellipse in Fig. 1a.

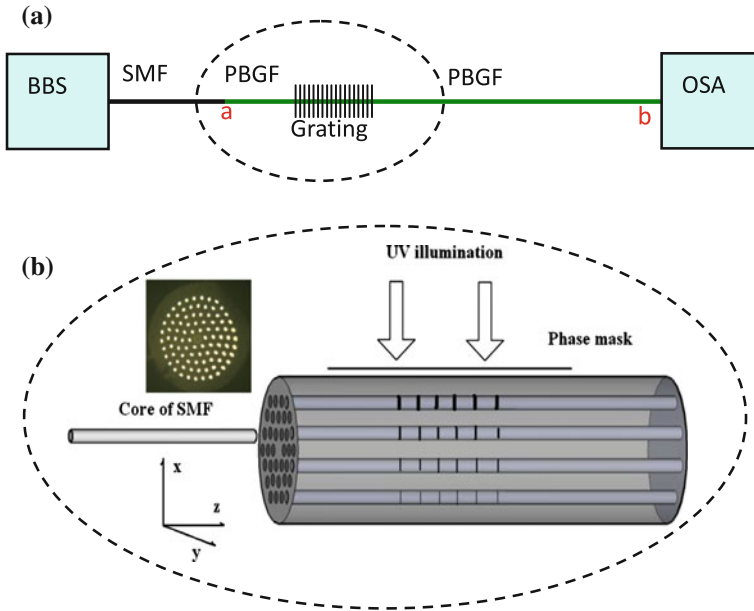


Fig. 1 **a** The schematic diagram of the experimental setup. **b** The schematic diagram of the blow up of the section circled by the *dotted ellipse* in Fig. 1a. The *right part* is the fiber Bragg grating inscribed into the high-index Ge-doped rods by UV illumination using phase mask. The *left part* is the core of the SMF transporting the light from BBS into the individual rod of the cladding of the all-solid PBGF

3 Experimental Realization and Analysis

Figure 2a shows the transmission spectra when the light is launched into the core and the six rods of the first ring (see the inset) of the all-solid PBGF after FBG fabrication. It is obviously seen that no Bragg resonance dip appears when the light is launched into the core of the PBGF. While Bragg resonance dips occur if the light is separately launched into the six rods of the first ring of the all-solid PBGF. The resonance wavelength of each rod is different. This is because each rod experienced different pulse energies due to the different vertical distances from the phase mask to the rod, and the index modulation for the rods is different resulting in different effective indices of the coupled modes n_{eff} for the rods. Hence, according to the fiber Bragg grating phase matching condition $\lambda_{res} = 2n_{eff} \Lambda$, where λ_{res} is the Bragg resonant wavelength and Λ is the period of the FBG, the resonant wavelengths are different. Since the above-mentioned experiment is based on that the light is first passing through the shorter length of the all-solid PBGF (as shown in Fig. 1a), for the convenience of description, we call the situation forward-launching.

Then, we launch the light into the core and the same rods from the right end of the all-solid PBGF, i.e., the b point as shown in Fig. 1a, and the OSA is connected with the left end. We call the situation back-launching. The transmission spectra are shown in

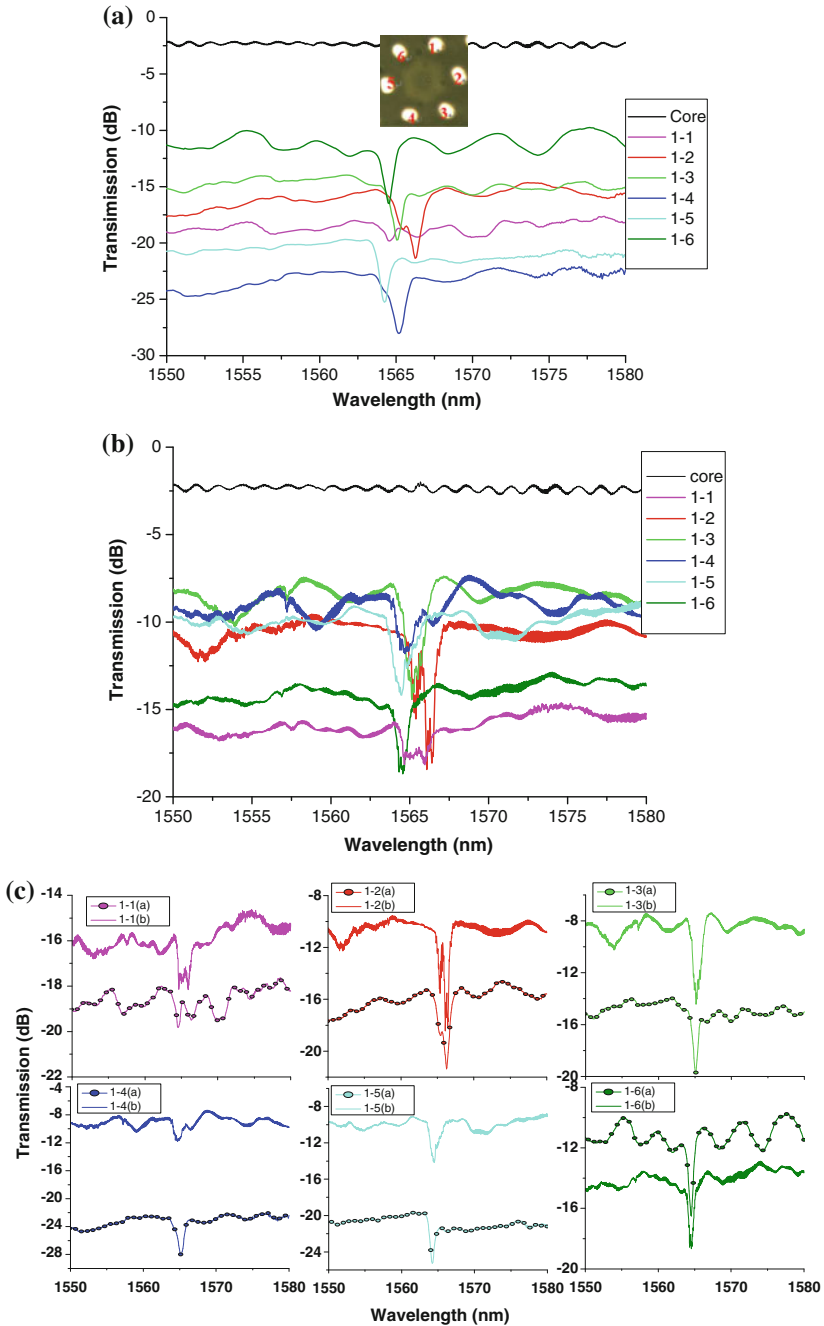
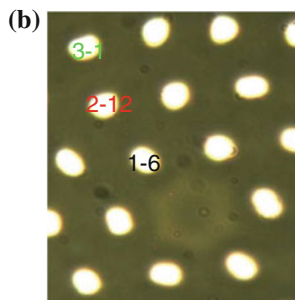
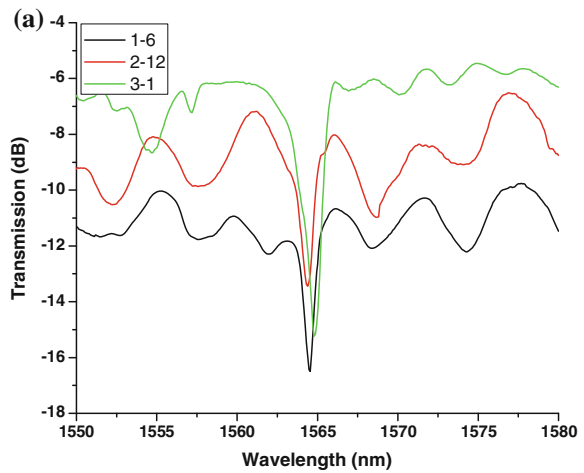


Fig. 2 The transmission spectra of the FBGs from the core and the six rods in the first ring of the all-solid PBGF after FBG fabrication for the two situations: **a** light forward-launching and **b** light back-launching. **c** Comparison of the transmission spectrum of the FBG from the same rod for the two situations: forward-launching (*dotted lines*) and back-launching (*solid lines*)

Fig. 2b. Similarly, there is no resonance dip if light is coupled into the core of the PBGF, and Bragg resonance dips with different resonance wavelengths and resonance widths also occur if the light is launched into the six rods of the first ring of the PBGF.

For comparison, we depict the transmission spectra of the FBG from the same rod for the two situations: forward-launching and back-launching, as shown in Fig. 2c. We can observe the transmission spectra of the FBGs from the same rod for the two situations have similar resonant wavelength. However, for the back-launching, the curves are not enough smooth. This is because, for the back-launching, light is first coupled into the rods of the longer length PBGF section, and the couplings between the adjacent rods occur. Then the coupled light in some rods is traveling through the FBG, and the transmission spectrum is not only simple Bragg resonance dips of the single rod, and they consist of the resonance dips of the adjacent rods. On contrary, for the forward-launching, the light is coupled into the shorter length PBGF section, which is short enough to couple the light between the adjacent rods and the light is restricted in the single rod. When the light travels through the FBG, the transmission spectrum is formed by the Bragg resonance dips of the single rod. Hence its resonance width is larger than the former situation (see the first figure in Fig. 2c). We also observe the transmission spectrum of the FBG from the rods of the second and the third ring, as shown in Fig. 3. The resonant dips from every rod are also

Fig. 3 **a** The transmission spectra of the FBG from three rods from the first, second and third rings, respectively. **b** The relative position of the three rods



obviously observed with different resonant wavelengths. In our experiments, the resonance wavelength width is larger than the Bragg resonance width in ordinary single mode fiber (SMF); this is because the mode couplings in the rods of the PBGF occur between the rods-guided supermodes, not the simple guided fundamental mode in the core of the SMF.

4 Conclusion

In conclusion, we realize the fiber Bragg grating arrays by inscribing into the Ge-doped cladding rods of an all-solid PBG hydrogen loaded fiber using KrF excimer laser. We launch the light into the Ge-doped rods from two reverse directions, and different resonance wavelengths and resonance widths are observed. The diverse resonance dips from different rods may have different responses to the environment changes, hence the fiber Bragg grating arrays will have good capacity to be employed as the multi-parameter sensor. If we control the length of the all-solid PBGF before the FBG, we may realize diverse resonance dips, and the fiber Bragg grating arrays can be used to study the properties of the supermode coupling in the rods. Still, there should be further research on the specific mode couplings in the rods of all-solid PBGF and in the FBG.

Acknowledgments This work was supported by the National Natural Science Foundation of China under Grant No. 11404240, and by the Doctoral Scientific Foundation of Tianjin Normal University under No. 52XB1307. The authors would like to thank Yangtze Optical Fiber and Cable Co. LTD (Wuhan, China) for providing PCFs.

References

1. Russell P (2003) Photonic crystal fibers. *Science* 299(5605):358–362
2. Knight JC (2003) Photonic crystal fibres. *Nature* 424(6950):847–851
3. Luan F (2004) All-solid photonic bandgap fiber. *Opt Lett* 29:2369–2371
4. Jin L (2007) Bragg grating resonances in all-solid bandgap fibers. *Opt Lett* 32:2717–2719
5. Jin L (2007) Spectral characteristics and bend response of Bragg gratings inscribed in all-solid bandgap fibers. *Opt Express* 15:15555–15565
6. Bigot L (2009) Efficient fiber Bragg gratings in 2D all-solid photonic bandgap fiber. *Opt Express* 17:10105–10112
7. Cook K (2010) Bragg gratings in Yb³⁺-doped solid photonic bandgap fibre, OSA